Journal of Sound and Vibration 329 (2010) 5307–5320

Contents lists available at ScienceDirect

Journal of Sound and Vibration

journal homepage: www.elsevier.com/locate/jsvi

A unified approach for predicting sound radiation from baffled rectangular plates with arbitrary boundary conditions

Xuefeng Zhang, Wen L. Li *

Department of Mechanical Engineering, Wayne State University, 5050 Anthony Wayne Drive, Detroit, MI 48202-3902, USA

ARTICLE INFO

Article history:
Received 5 August 2009
Received in revised form
9 July 2010
Accepted 13 July 2010
Handling Editor: R.E. Musafir

ABSTRACT

This paper discusses sound radiation from a baffled rectangular plate with each of its edges arbitrarily supported in the form of elastic restraints. The plate displacement function is universally expressed as a 2-D Fourier cosine series supplemented by several 1-D series. The unknown Fourier expansion coefficients are then determined by using the Rayleigh–Ritz procedure. Once the vibration field is solved, the displacement function is further simplified to a single standard 2-D Fourier cosine series in the subsequent acoustic analysis. Thus, the sound radiation from a rectangular plate can always be obtained from the radiation resistance matrix for an invariant set of cosine functions, regardless of its actual dimensions and boundary conditions. Further, this radiation resistance matrix, unlike the traditional ones for modal functions, only needs to be calculated once for all plates with the same aspect ratio. In order to determine the radiation resistance matrix effectively, an analytical formula is derived in the form of a power series of the non-dimensional acoustic wavenumber; the formula is mathematically valid and accurate for any wavenumber. Several numerical examples are presented to validate the formulations and show the effect of the boundary conditions on the radiation behavior of planar sources.

1. Introduction

Plates are one of the most widely used structural components in industrial applications. Acoustic radiation from plates with various boundary conditions and/or loading features (e.g., masses, springs, dampers, ribs, etc.) is of great interest to both researchers and practicing engineers since the sound radiated from a plate can be meaningfully reduced by altering the relative amplitudes of the vibration modes [1] or by modifying the boundary support configurations [2]. From the standpoint of noise control, however, the structural modes which dominate the structural vibrations are not necessarily responsible for the acoustic responses [3], and a more restrained plate does not always have higher radiation efficiency as is commonly believed [4]. Thus, a better understanding of the effects of the boundary condition on sound radiation is both technically and practically relevant.

It is well known that an infinite plate can radiate sound only if its structural wavenumber is smaller than the acoustic wavenumber, and the radiation efficiency can be readily calculated from simple formulas [5]. In contrast, a plate of finite dimensions can theoretically radiate sound at any given wavenumber. However, its radiation efficiency can vary substantially depending on the ratio of the acoustic to structural wavenumbers [6]. Wavenumber space is often divided into several regions with reference to the coincident frequency. In the above-coincidence region, simple formulas derived

* Corresponding author. Tel.: +1 313 577 3875.
E-mail address: wli@wayne.edu (W.L. Li).

0022-460X/$ - see front matter © 2010 Elsevier Ltd. All rights reserved.
doi:10.1016/j.jsv.2010.07.014

for an infinite plate are good approximations. In the below-coincidence region, the acoustic characteristics of plates can be understood from the truncation of wave forms at the edges [7]. Due to more cancellation in the truncated wave forms, even modes tend to be less efficient than odd modes in radiating sound [3,5]. The edge or corner effects can be conveniently used to qualitatively explain the modal radiation characteristics of a simply supported plate. Although the radiation behavior may not be so easily described for plates with other more complicated boundary conditions, it can be generally said that boundary conditions play a critical role in affecting sound radiation in the below-coincidence frequency region.

The sound radiation from a simply supported rectangular plate has been extensively studied for many years [1,3,5,6,8–16]. Two general approaches are often used in calculating the radiated sound power. In the first approach, the radiated power is calculated by integrating the sound intensity over the plate surface [6]. In the second approach, the radiated power is determined based on the far-field pressure on a hemisphere of sufficiently large radius [9]. Regardless of which approach is employed, the analysis will typically involve the calculation of multiple surface integrals, which is often carried out numerically and represents the most time-consuming part of an acoustic analysis. Many simplified, approximate or asymptotic formulas have been derived to reduce the computing burden. However, they are typically only applicable to the frequency ranges well below or well above the coincidence frequency [5,10,17]. Exact analytical expressions in the form of series expansion were recently derived for the radiation resistances of a simply supported plate [15]. Although this set of equations is theoretically applicable for any frequency, it is most effective only in the low- to mid-frequency ranges.

Sound radiation from plates has also been studied for other boundary conditions. A clamped plate was found to be almost twice as effective in radiating sound as its simply supported counterpart [10]. In particular, a 3-dB correction is often applied to a clamped plate for frequencies up to half of the critical frequency [5,18] and then is progressively reduced to unity at the critical frequency. This trend was also predicted for high modal numbers by studying a semi-infinite plate with an elastic edge restraint against rotation [17]. The analysis, however, cannot be easily extended to the so-called corner modes because of the non-separable nature of the plate problem. The analytical expressions were later used to calculate the modal-averaged correction factors of the edge modes in studying the effects of the boundary constraints and the angles of the baffles [19]. Radiation from simply supported plates with rotational elastic restraints was also studied [20,21]. It is widely believed that adding rotational restraints to an edge of a simply supported plate tends to increase its radiation efficiency [17,18]. It was observed, however, that a plate with greater edge constraints does not necessarily have higher radiation efficiency [4,21,22]. A trigonometric series expansion method was previously used to study the vibration [23] of and the acoustic radiation [24] from plates with arbitrary boundary conditions that actually refer to the cases where the classical homogeneous boundary conditions (i.e., free, clamped, simply supported and guided) can be specified differently from one edge to another. Several supplementary terms were added to the trigonometric series so that the essential boundary conditions can be readily satisfied by including/excluding some of them.

In this study, an analytical method was developed for the acoustic radiation from a rectangular plate with elastic restraints against both deflection and rotation along the edges. The plate displacement function was universally expressed as a two-dimensional Fourier cosine series supplemented with several one-dimensional series which were introduced to deal with the potential convergence difficulties (with the conventional Fourier method) when a plate is generally supported [25]. In this way, the radiation behavior of a plate, regardless of its boundary conditions, can be easily derived from the radiation resistances for a complete set of invariants (cosine functions). One of the immediate advantages is that relatively time-consuming acoustic calculations now need to be carried out only once when a plate is subjected to various structural modifications.

This paper is structured as follows: in Section 2 an analytical method is first briefly reviewed for the vibration analysis of a plate with general elastic restraints along the edges. It is shown in Section 3 that the radiation behavior of the plate can be determined from the radiation resistances for a complete set of cosine functions, and a new formula is derived for analytically calculating the radiation resistance matrix for this set of invariants. In Section 4, numerical examples concerning the modal radiation efficiencies of plates and their sound power radiation under various boundary conditions are presented.

2. Vibration of a rectangular plate

Fig. 1 shows a rectangular plate with elastic restraints against both deflection and rotation along its edges. The plate is considered so thin that the effects of both the rotary inertia and the transverse shear deformation can be neglected.

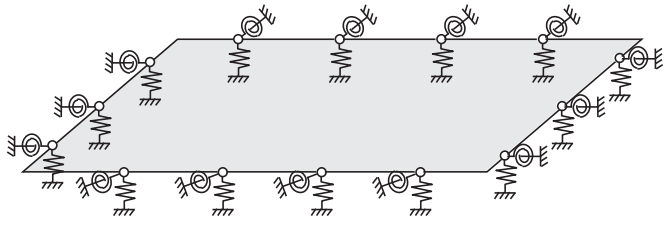

Fig. 1. A rectangular plate with arbitrary elastic restraints at its edges.

The vibration of the plate is governed by the following differential equation:

$$D\nabla^4 w(x,y)-\rho h\omega^2 w(x,y)=f(x,y), \tag{1}$$

where $\nabla^4=\partial^4/\partial x^4+2\partial^4/\partial x^2\partial y^2+\partial^4/\partial y^4$, $w(x, y)$ is the flexural displacement; ω is the angular frequency; D, ρ, and h are the bending rigidity, the mass density and the thickness of the plate, respectively; and $f(x, y)$ is the distributed harmonic excitation acting on the plate surface. The time-dependent term $e^{i\omega t}$ is suppressed in Eq. (1) for simplicity.

The boundary conditions along the elastically restrained edges can be specified as

$$k_{x_0}(y)w=Q_x,\quad K_{x_0}(y)\partial w/\partial x=-M_x\quad \text{at } x=0, \tag{2, 3}$$

$$k_{x_a}(y)w=-Q_x,\quad K_{x_a}(y)\partial w/\partial x=M_x\quad \text{at } x=a, \tag{4, 5}$$

$$k_{y_0}(x)w=Q_y,\quad K_{y_0}(x)\partial w/\partial y=-M_y\quad \text{at } y=0, \tag{6, 7}$$

and

$$k_{y_b}(x)w=-Q_y,\quad K_{y_b}(x)\partial w/\partial y=M_y\quad \text{at } y=b, \tag{8, 9}$$

where $k_{x_0}(y)$, $k_{x_a}(y)$, $k_{y_0}(x)$, and $k_{y_b}(x)$ are the stiffness functions for the linear elastic restraints; $K_{x_0}(y)$, $K_{x_a}(y)$, $K_{y_0}(x)$, and $K_{y_b}(x)$ are the stiffness functions for the rotational restraints; and Q_x, Q_y, M_x, and M_y are the shear forces and bending moments at the edges. It should be noted that the stiffness for each elastic restraint is allowed to vary with length. Eqs. (2)–(9) describe a general set of boundary conditions; all the classical boundary conditions (free, simply supported, clamped, guided, and the combinations) can be simply specified as special cases when the stiffness for each of the elastic restraints is equal either to zero or to infinity.

The plate displacement will be invariably expressed here as a modified Fourier series expansion in the form of [25]

$$w(x,y)=\sum_{m=0}^{\infty}\sum_{n=0}^{\infty}A_{mn}\cos\lambda_{am}x\cos\lambda_{bn}y+\sum_{j=1}^{4}\left(\xi_b^j(y)\sum_{m=0}^{\infty}c_m^j\cos\lambda_{am}x+\xi_a^j(x)\sum_{n=0}^{\infty}d_n^j\cos\lambda_{bn}y\right) \tag{10}$$

where $\lambda_{am}=m\pi/a$, $\lambda_{bn}=n\pi/b$, and $\xi_a^j(x)$ (or $\xi_b^j(y)$) denote a set of closed-form functions defined as

$$\xi_a^1(x)=\frac{9a}{4\pi}\sin\left(\frac{\pi x}{2a}\right)-\frac{a}{12\pi}\sin\left(\frac{3\pi x}{2a}\right),\quad \xi_a^2(x)=-\frac{9a}{4\pi}\cos\left(\frac{\pi x}{2a}\right)-\frac{a}{12\pi}\cos\left(\frac{3\pi x}{2a}\right), \tag{11, 12}$$

$$\xi_a^3(x)=\frac{a^3}{\pi^3}\sin\left(\frac{\pi x}{2a}\right)-\frac{a^3}{3\pi^3}\sin\left(\frac{3\pi x}{2a}\right),\quad \xi_a^4(x)=-\frac{a^3}{\pi^3}\cos\left(\frac{\pi x}{2a}\right)-\frac{a^3}{3\pi^3}\cos\left(\frac{3\pi x}{2a}\right). \tag{13, 14}$$

Augmenting the standard Fourier series with the extra terms is to recognize the fact that the Fourier series of a smooth function $f(x)$ on a compact interval $[0, a]$ usually exhibits slow convergence (or, even, fails to converge) due to possible jumps at the interval endpoints after the periodic extension of the function. The 1-D Fourier series expansions in Eq. (10) are used here to represent the first and third derivatives of the displacement function along the edges of the plate. By doing so, the 2-D series now actually represents a residual displacement function that has at least three continuous derivatives with respect to both the x and y coordinates when periodically extended onto the entire x–y plane. According to the convergence theorem [26], the convergence (rate) for the Fourier series expansion of a periodic function is proportional to the degree of smoothness of the function. Therefore, the series expression in Eq. (10) is guaranteed to converge at a substantially improved speed for any boundary conditions. As a matter of fact, polynomial subtractions have long been used by mathematicians as a means to accelerate the convergence of the Fourier series expansion for a given function [27–29].

The series expansion in Eq. (10) may appear to be similar to that previously used in Refs. [23,24]. However, there are some significant differences between that series expansion and the current one. First, the supplementary terms there are used to account for the possible non-zero displacement and rotation at an edge, rather than the first and third derivatives as in Eq. (10). From a mathematical point of view, the inclusion of the rotation terms will not help to improve the convergence of the sine series expansion. Second, each of the regular trigonometric functions ($m\geq 5$) has zero displacement and zero slope at both ends, and the resultant series is essentially a standard Fourier sine series multiplied by the window function $\sin(\pi x/a)$. While such a treatment easily ensures that the essential boundary conditions are satisfied by the admissible functions, the window function tends to infinitely amplify the error at or near an edge. This may explain the slight lack of precision near the edges and as much as a 1.5% error in the calculated eigenfrequencies for a simply supported plate [23].

Other important mathematical features for the series expression in Eq. (10) are directly related to its completeness, differentiability, and suitability for constructing a strong form of solution. The completeness of the trigonometric functions mathematically ensures that the series in Eq. (10) is able to expand *any* function $f(x, y)\in C^3$, $\forall(x, y)\in([0, a]\otimes[0, b])$. In addition, this series can be differentiated, term-by-term, to obtain the uniformly convergent series expansions for up to the fourth-order derivatives of the function $f(x, y)$ in the x or y directions. Thus, the series solution is exact if it is sought to simultaneously satisfy the governing differential equation at *every* field point and the boundary conditions at *every*

boundary point [25]. Alternatively, the solution can also be found in a weak form by using, for example, the Rayleigh–Ritz method. The weak formulation is considered advantageous for extending this work to complicated structures.

Unlike in the strong formulation, all the Fourier coefficients will be treated as mutually independent generalized coordinates and solved directly from the minimization of Hamilton's function

$$H(w)=T(w)-V(w)+W(w), \tag{15}$$

where $T(w)$ is the total kinetic energy, $V(w)$ is the total potential energy, and $W(w)$ is the work done by the excitation force.

For a purely bending plate, the total potential energy, kinetic energy and external work can be, respectively, expressed as

$$\begin{aligned} V(w)=\frac{D}{2}\int_0^a\int_0^b\left[(\partial^2 w/\partial x^2)^2+(\partial^2 w/\partial y^2)^2+2\nu\partial^2 w/\partial x^2\partial^2 w/\partial y^2+2(1-\nu)(\partial^2 w/\partial x\partial y)^2\right]\mathrm{d}x\,\mathrm{d}y\\ +1/2\int_0^b(k_{x_0}w^2+K_{x_0}(\partial w/\partial x)^2)_{x=0}\,\mathrm{d}y+1/2\int_0^b(k_{x_a}w^2+K_{x_a}(\partial w/\partial x)^2)_{x=a}\,\mathrm{d}y\\ +1/2\int_0^a(k_{y_0}w^2+K_{y_0}(\partial w/\partial y)^2)_{y=0}\,\mathrm{d}x+1/2\int_0^a(k_{y_b}w^2+K_{y_b}(\partial w/\partial y)^2)_{y=b}\,\mathrm{d}x, \end{aligned} \tag{16}$$

$$T(w)=\frac{1}{2}\int_0^a\int_0^b\rho h(\partial w/\partial t)^2\,\mathrm{d}x\,\mathrm{d}y, \tag{17}$$

and

$$W(w)=\int_0^a\int_0^b f(x,y)w(x,y)\,\mathrm{d}x\,\mathrm{d}y. \tag{18}$$

In Eq. (16), the first integral represents the strain energy due to the bending of the plate, and the other integrals represent the potential energies stored in the restraining springs.

In order to be able to account for the arbitrariness of the stiffness distribution for each elastic restraint, the stiffness functions will be expanded into simple Fourier cosine series [30], for example

$$k_{x_0}(y)=\sum_{l=0}^{\infty}\tilde{k}_{x_0,l}\cos\left(\frac{l\pi}{b}y\right). \tag{19}$$

where $\tilde{k}_{x_0,l}$ is the Fourier coefficients of the Fourier cosine series expansion of the stiffness function $k_{x0}(y)$ along $x=0$.

It can be proved mathematically that the cosine series expansion of any continuous stiffness function will converge at a rate of, at least, $(l\pi)^2$.

Minimization of the Hamiltonian function will lead to the following system of equations:

$$\sum_{m'=0}^{\infty}\sum_{n'=0}^{\infty}K^{11}_{mn,m'n'}A_{m'n'}+\sum_{j=1}^{4}\sum_{m'=0}^{\infty}K^{12}_{mn,jm'}c^j_{m'}+\sum_{j=1}^{4}\sum_{n'=0}^{\infty}K^{13}_{mn,jn'}d^j_{n'}-\rho h\omega^2\Delta_m\Delta_n\left[A_{mn}+\sum_{j=1}^{4}\tilde{\beta}^j_n c^j_m+\sum_{j=1}^{4}\tilde{\alpha}^j_m d^j_n\right]=f_{mn} \tag{20}$$

$$\sum_{m'=0}^{\infty}\sum_{n'=0}^{\infty}K^{21}_{im,m'n'}A_{m'n'}+\sum_{j=1}^{4}\sum_{m'=0}^{\infty}K^{22}_{im,jm'}c^j_{m'}+\sum_{j=1}^{4}\sum_{n'=0}^{\infty}K^{23}_{im,jn'}d^j_{n'}-\rho h\omega^2\Delta_m\left[\sum_{n'=0}^{\infty}\left(A_{mn'}+\sum_{j=1}^{4}\tilde{\alpha}^j_m d^j_{n'}\right)\beta^i_{n'}+\sum_{j=1}^{4}\beta^{0,0}_{i,j}c^j_m\right]=f^i_{am} \tag{21}$$

and

$$\sum_{m'=0}^{\infty}\sum_{n'=0}^{\infty}K^{31}_{in,m'n'}A_{m'n'}+\sum_{j=1}^{4}\sum_{m'=0}^{\infty}K^{32}_{in,jm'}c^j_{m'}+\sum_{j=1}^{4}\sum_{n'=0}^{\infty}K^{33}_{in,jn'}d^j_{n'}-\rho h\omega^2\Delta_n\left[\sum_{m'=0}^{\infty}\left(A_{m'n}+\sum_{j=1}^{4}\tilde{\beta}^j_n c^j_{m'}\right)\alpha^i_{m'}+\sum_{j=1}^{4}\alpha^{0,0}_{i,j}d^j_n\right]=f^i_{bn} \tag{22}$$

By truncating all the series expansions to $m=M$ and $n=N$, Eqs. (20)–(22) can be rewritten in matrix form as

$$\begin{bmatrix}K^{11}_{mn,m'n'} & K^{12}_{mn,jm'} & K^{13}_{mn,jn'}\\ K^{21}_{im,m'n'} & K^{22}_{im,jm'} & K^{23}_{im,jn'}\\ K^{31}_{in,m'n'} & K^{32}_{in,jm'} & K^{33}_{in,jn'}\end{bmatrix}\begin{bmatrix}A_{mn}\\ c^i_m\\ d^i_n\end{bmatrix}-\rho h\omega^2\begin{bmatrix}M^{11}_{mn,m'n'} & M^{12}_{mn,jm'} & M^{13}_{mn,jn'}\\ M^{21}_{im,m'n'} & M^{22}_{im,jm'} & M^{23}_{im,jn'}\\ M^{31}_{in,m'n'} & M^{32}_{in,jm'} & M^{33}_{in,jn'}\end{bmatrix}\begin{bmatrix}A_{mn}\\ c^i_m\\ d^i_n\end{bmatrix}=\begin{bmatrix}f_{mn}\\ f^i_{am}\\ f^i_{bn}\end{bmatrix} \tag{23}$$

The new symbols, $K^{11}_{mn,m'n'}$, $M^{11}_{mn,m'n'}$, etc., denote the sub-matrices of the stiffness and mass matrices, respectively. The detailed expressions of these matrices and the force terms on the right hand side of Eqs. (20)–(22) are all given in Appendix A.

For a given excitation, $\mathbf{f}\neq\mathbf{0}$, all the unknown expansion coefficients and, hence, the response of the plate can be directly solved from Eq. (23). By letting $\mathbf{f}=\mathbf{0}$, Eq. (23) simply reduces to a familiar characteristic equation, and all the eigenpairs can be readily determined by solving a standard matrix eigenvalue problem.

3. Sound radiation from an arbitrarily supported plate

For a baffled vibrating plate, the total radiated acoustic power can be calculated from

$$W = \frac{1}{2}\iint_S \mathrm{Re}[\dot{w}^*(x,y)p(x,y)]\,\mathrm{d}x\,\mathrm{d}y \tag{24}$$

where $p(x, y)$ is the sound pressure on the plate surface, $\dot{w}(x,y)$ is the normal velocity of the vibrating plate, and Re and * denote the real part and the complex conjugate of a complex number, respectively.

The sound pressure on the plate surface can be determined from the Rayleigh integral

$$p(x,y) = -\frac{\mathrm{i}\omega\rho_0}{2\pi}\int_0^b\int_0^a \frac{\dot{w}(x',y')e^{\mathrm{i}kR}}{R}\,\mathrm{d}x'\,\mathrm{d}y' \tag{25}$$

where k is the acoustic wavenumber, ρ_0 is the density of the acoustic media, and $R = \sqrt{(x-x')^2+(y-y')^2}$.

The radiation resistance is defined as

$$R_{\mathrm{rad}} = W/\langle \dot{w}^2 \rangle, \tag{26}$$

where $\langle \dot{w}^2 \rangle$ is the mean-square velocity averaged with respect to both time and space, namely

$$\langle \dot{w}^2 \rangle = \frac{1}{2S}\int_S [\dot{w}(x,y)]^2\,\mathrm{d}S. \tag{27}$$

where S is the surface area of the plate.

In practice, the radiation resistance is often replaced by a non-dimensional quantity, the so-called radiation efficiency, defined as

$$\sigma = R_{\mathrm{rad}}/(\rho_0 cS). \tag{28}$$

where c is the speed of sound.

In order to simplify the acoustic calculations, all the supplementary functions in Eq. (10) will be expanded into Fourier cosine series. Thus, the displacement function reduces to

$$w(x,y) = \sum_{m=0}^{\infty}\sum_{n=0}^{\infty}\overline{A}_{mn}\cos\lambda_{am}x\cos\lambda_{bn}y, \tag{29}$$

where $\overline{A}_{mn} = A_{mn} + \sum_{l=1}^{4}(\tilde{\beta}_n^l c_m^l + \tilde{\alpha}_m^l d_n^l)$.

It should be noted that the Fourier series expansion for each supplementary function converges at a speed of $(m\pi)^2$, the same as that for the displacement solution. Thus, the acoustic and structural solutions are numerically compatible in terms of their accuracy and convergence.

In light of Eq. (29), the radiated power will generally depend on (a) the self-radiation resistance corresponding to each term in the series expansion as if it were the only term there and (b) the mutual radiation resistances resulting from its cross-couplings with the other terms. By substituting Eqs. (25) and (29) into Eq. (24), the sound power radiated from the plate can be expressed as

$$W = \frac{1}{2}ab\rho_0 c\omega^2\overline{\mathbf{A}}^H\Xi\overline{\mathbf{A}}, \tag{30}$$

where the superscripted H denotes the Hermitian operation and the elements of the specific radiation resistance matrix, Ξ, are defined as

$$\xi_{mn,m'n'} = \frac{2k}{\pi ab}\int_0^b\int_0^a\int_0^b\int_0^a \cos\lambda_{am}x\cos\lambda_{bn}y\cos\lambda_{am'}x'\cos\lambda_{bn'}y'\frac{\sin k\sqrt{(x-x')^2+(y-y')^2}}{\sqrt{(x-x')^2+(y-y')^2}}\,\mathrm{d}x'\,\mathrm{d}y'\,\mathrm{d}x\,\mathrm{d}y \tag{31}$$

The radiation efficiency for a mode can be calculated from

$$\sigma = \left(\frac{\overline{\mathbf{A}}^l}{|\overline{\mathbf{A}}^l|}\right)^H \Xi \left(\frac{\overline{\mathbf{A}}^l}{|\overline{\mathbf{A}}^l|}\right), \tag{32}$$

where

$$|\overline{\mathbf{A}}^l| = \left[\sum_{m=0}^{M}\sum_{n=0}^{N}(1+\delta_{m0})(1+\delta_{n0})\left(\overline{A}_{mn}^l\right)^2\right]^{1/2}$$

with δ_{mn} being the Kronecker delta.

By introducing a new set of coordinates $\kappa=x-x'$, $\tau=y-y'$, $\varsigma=x+x'$, $\gamma=y+y'$, one can reduce the quadruple integral in Eq. (31) to a double integral as

$$\xi_{mn,m'n'}=\frac{2k}{\pi ab}\int_0^b\int_0^a X(\kappa)Y(\tau)\frac{\sin k\sqrt{\kappa^2+\tau^2}}{\sqrt{\kappa^2+\tau^2}}\,\mathrm{d}\kappa\,\mathrm{d}\tau, \tag{33}$$

where

$$X(\kappa)=\begin{cases}(a-\kappa)\cos\lambda_{am}\kappa+\dfrac{1}{\lambda_{am}}\sin\lambda_{am}\kappa & (m=m'),\\ \dfrac{1+(-1)^{m+m'}}{\lambda_{am}^2-\lambda_{am'}^2}(\lambda_{am}\sin\lambda_{am'}\kappa-\lambda_{am'}\sin\lambda_{am}\kappa) & (m\neq m')\end{cases} \tag{34}$$

and

$$Y(\tau)=\begin{cases}(b-\tau)\cos\lambda_{bn}\tau+\dfrac{1}{\lambda_{bn}}\sin\lambda_{bn}\tau & (n=n'),\\ \dfrac{1+(-1)^{n+n'}}{\lambda_{bn}^2-\lambda_{bn'}^2}(\lambda_{bn}\sin\lambda_{bn'}\tau-\lambda_{bn'}\sin\lambda_{bn}\tau) & (n\neq n').\end{cases} \tag{35}$$

Various approximate, asymptotic, or numerical techniques have been employed in the literature to calculate the integrals in Eqs. (31) and (33) in different frequency regimes. In this study, a new analytical formula will be derived by following the procedure which was previously developed for modeling sound radiation from a simply supported plate [15].

Making use of the MacLaurin series expansion [31], one has

$$\frac{\sin kR}{R}=\sum_{p=0}^{\infty}\frac{(-1)^p(kR)^{2p+1}}{R(2p+1)!}=\sum_{p=0}^{\infty}\frac{(-1)^pk^{2p+1}R^{2p}}{(2p+1)!}\quad(R=\sqrt{x^2+y^2}) \tag{36}$$

and

$$R^{2p}=(x^2+y^2)^p=\sum_{q=0}^{p}\frac{p!}{q!(p-q)!}x^{2p-2q}y^{2q}. \tag{37}$$

Substituting Eqs. (36) and (37) into (33) results in

$$\xi_{mn,m'n'}=\frac{2k}{\pi ab}\sum_{p=0}^{\infty}\sum_{q=0}^{p}\frac{p!}{q!(p-q)!}\frac{(-1)^pk^{2p+1}}{(2p+1)!}\int_0^a\kappa^{2p-2q}X(\kappa)\,\mathrm{d}\kappa\int_0^b\tau^{2q}Y(\tau)\,\mathrm{d}\tau \tag{38}$$

In light of Eq. (34), the integrals, for example, $\int_0^a\kappa^{2p}X_{mm'}(\kappa)\,\mathrm{d}\kappa$, can be rewritten as

$$\begin{aligned}\int_0^a\kappa^{2p}X_{mm'}(\kappa)\,\mathrm{d}\kappa&=a^{2p+2}\int_0^1\chi^{2p}\left(\frac{1+(-1)^{m+m'}}{\pi(m^2-m'^2)}[m\sin m'\pi\chi-m'\sin m\pi\chi]\right)\mathrm{d}\chi\quad(m\neq m')\\&=a^{2p+2}\left(\frac{1+(-1)^{m+m'}}{\pi(m^2-m'^2)}\left[mS_{2p}^{m'}-m'S_{2p}^{m}\right]\right),\end{aligned} \tag{39}$$

where

$$S_p^m=\int_0^1x^p\sin(m\pi x)\,\mathrm{d}x \tag{40}$$

simply represent a list of mathematical constants for $m=1, 2, \ldots$, and $p=1, 2, \ldots$

For $m=m'$,

$$\begin{aligned}\int_0^a\kappa^{2p}X_{mm}(\kappa)\,\mathrm{d}\kappa&=a^{2p+2}\int_0^1\chi^{2p}\left((1-\chi)\cos m\pi\chi+\frac{1}{m\pi}\sin m\pi\chi\right)\mathrm{d}\chi\\&=a^{2p+2}\left[\int_0^1\chi^{2p}\cos m\pi\chi\,\mathrm{d}\chi-\int_0^1\chi^{2p+1}\cos m\pi\chi\,\mathrm{d}\chi+\frac{1}{m\pi}\int_0^1\chi^{2p}\sin m\pi\chi\,\mathrm{d}\chi\right]\\&=a^{2p+2}\left[\frac{\sin m\pi\chi}{m\pi}\chi^{2p}\Big|_0^1-\frac{1}{m\pi}\int_0^1 2p\chi^{2p-1}\sin m\pi\chi\,\mathrm{d}\chi\right.\\&\left.-\frac{\sin m\pi\chi}{m\pi}\chi^{2p+1}\Big|_0^1+\frac{1}{m\pi}\int_0^1(2p+1)\chi^{2p}\sin m\pi\chi\,\mathrm{d}\chi+\frac{1}{m\pi}S_{2p}^m\right]\\&=\frac{a^{2p+2}}{m\pi}\left[(2p+2)S_{2p}^m-2pS_{2p-1}^m\right].\end{aligned} \tag{41}$$

The τ-related integrals can be calculated in the same manner.

Making use of Eqs. (39) and (41), Eq. (38) can be eventually expressed as

$$\xi_{mn,m'n'} = \frac{2}{\pi}\sum_{p=0}^{\infty}\sum_{q=0}^{p}\frac{p!}{q!(p-q)!}\frac{(-1)^p(ka)^{2p+2}r^{2q+1}}{(2p+1)!}U_{p-q}^{m,m'}U_{q}^{n,n'}, \tag{42}$$

where $r=a/b$ is the aspect ratio of the plate, and

$$U_p^{m,m'} = \begin{cases} \dfrac{2}{m\pi}((p+1)S_{2p}^{m}-pS_{2p-1}^{m}) & (m=m'), \\ \dfrac{1+(-1)^{m+m'}}{\pi(m^2-m'^2)}\left[mS_{2p}^{m'}-m'S_{2p}^{m}\right] & (m\neq m'). \end{cases} \tag{43}$$

In this way, the original surface integrations have been converted into the calculations of a set of simple integrals, S_p^m, which are evaluated analytically as [15]

$$S_{2p-1}^{m} = \sum_{j=1}^{p}\frac{(-1)^{m+j}(2p-1)!}{(2p-2j+1)!(m\pi)^{2j-1}} \tag{44}$$

and

$$S_{2p}^{m} = \sum_{j=1}^{p}\left\{\frac{(-1)^{m+j}(2p)!}{(2p-2j+2)!(m\pi)^{2j-1}}\right\}+(-1)^p\left[1-(-1)^m\right]\frac{(2p)!}{(m\pi)^{2p+1}}. \tag{45}$$

Eqs. (44) and (45) may become numerically unstable when p becomes very large. In such a case, for example, when $p>\max(m\pi,10)$, the following formula should be used instead:

$$S_{p}^{m} = \sum_{j=1}^{\infty}\frac{(-1)^{m+j}(m\pi)^{2j-1}p!}{(p+2j)!}. \tag{46}$$

Theoretically, Eq. (42) can be used to accurately calculate $\xi_{mn,m'n'}$ for any wavenumber. In practice, however, it will become less effective for large wavenumbers such as $ka>25$ because many terms have to be included in the series expansion and the numerical results are prone to be seriously contaminated by computer round-off errors. Fortunately, the radiation behavior of a plate tends to become very simple for large wavenumbers and can be well determined by some existing approximate or asymptotic formula. Thus, it is legitimate to limit the application of Eq. (42) to small to moderately large wavenumbers. It has been shown [15] that a formula similar to Eq. (42) can lead to a reduction of computing time by approximately three orders of magnitude as compared with the traditional numerical integration schemes.

In addition to being highly effective in computations, the technical and practical significances of the new formula, Eq. (42), should not be underestimated. First, Eq. (42), when combined with Eq. (30), can be generally used to predict the acoustic characteristics of rectangular plates which are arbitrarily supported along an edge and/or loaded with structural features like springs, masses and ribs. Practically, the radiation resistance matrix for a given plate needs to be calculated only once when its boundary conditions or loading features are modified. This is starkly different from the traditional modal-based approaches in which the acoustic calculations will have to be carried out repeatedly each time when a structural modification is made. Second, the current approach also provides a means for experimentally determining the radiation behavior of a planar source from the measured vibration data. In such a procedure, the Fourier expansion coefficients, instead of being analytically solved from Eq. (23), will be calculated from the spatial Fourier transform of the experimental displacement field, measured on the surface of the source. This essentially represents a hybrid analytical–experimental technique for determining the sound power radiation from a complex source.

4. Results and discussion

In this section, the new formulation will be first validated against some existing results in the literature. The modal radiation efficiency and radiated power are then presented for plates with various boundary conditions. In the following examples, the physical parameters are specified as $a=1$ m, $r=a/b=1.2$, $h=6\times10^{-3}$ m, $\rho=7800$ kg/m^3, $E=2.07\times10^{11}$ Pa, and $\nu=0.3$ for the plate and $\rho_0=1.2$ kg/m^3, and $c=340$ m/s for the acoustic medium.

4.1. Validation of the radiation efficiency calculations

The radiation efficiencies of plates with simply supported boundary conditions have been extensively studied in the literature. In comparison, few investigations have been devoted to the sound radiation from plates with other boundary conditions. As previously mentioned the proposed method offers a general and unified means for the acoustic analysis of plates with any boundary conditions. Under the current framework, the classical homogeneous boundary conditions can be simply viewed as the special cases when each elastic restraint is either extremely weak or strong. For example, a simply supported edge can be readily simulated by setting the stiffnesses of the transverse and rotational springs to infinity and

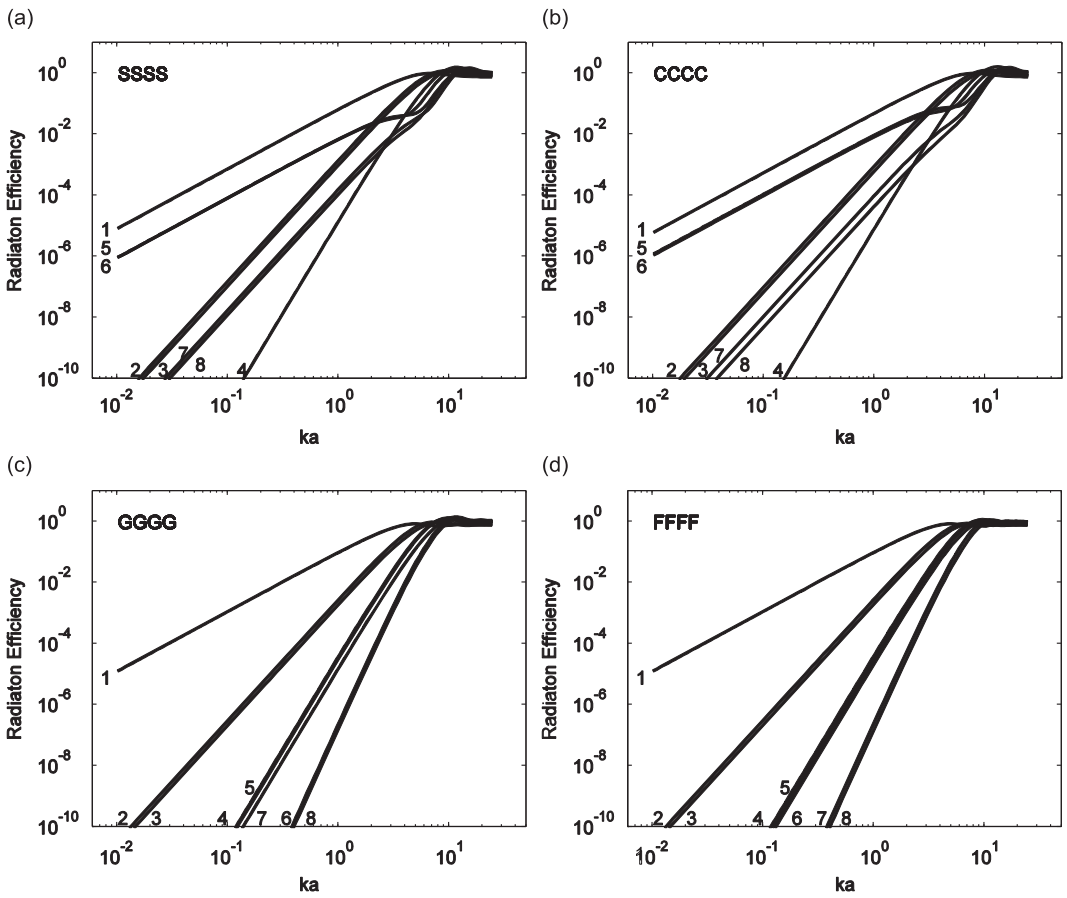

Fig. 2. Modal radiation efficiencies of a rectangular plate with aspect ratio r=1.2 and (a) simply supported, (b) clamped, (c) guided, and (d) free boundary conditions.

Table 1
Frequency parameters $\boldsymbol{\Omega} = \omega a^2\sqrt{\rho h/D}$ for rectangular plates with some classical boundary conditions and aspect ratio r=1.2.

Ω	1	2	3	4	5	6	7	8	9	10
FFFF	0.00	0.00	0.00	16.14	21.15	32.38	39.30	44.85	61.44	76.97
GGGG	0.00	9.87	14.21	24.08	39.48	53.69	56.85	66.72	88.83	96.33
SSSS	24.08	53.68	66.71	96.29	103.01	137.73	145.60	167.29	172.05	214.61
CFFF	3.47	9.77	21.46	34.22	36.57	60.77	66.02	73.60	92.05	110.62
CCFF	8.43	26.59	35.06	57.84	65.59	90.99	98.04	114.06	124.22	154.94
CCCF	24.84	48.93	64.17	89.65	103.16	123.16	142.62	149.48	187.12	201.81
CCCC	44.29	80.08	99.67	132.65	137.76	184.54	187.75	215.59	216.53	264.19

zero, respectively. Obviously, in actual numerical calculations, infinity needs to be represented by a sufficiently large number, and all the series expansions will be truncated to include only a finite number of terms, e.g., M=N=20.

In Fig. 2, the modal radiation efficiencies are plotted for the eight lowest modes of the plate under four different boundary conditions. These results were previously obtained, for example, by Wallace [10] for the simply supported (S) case, by Li [21] for the clamped (C) case, by Gomperts [4] and Berry et al. [7] for the guided (G) case, and by Berry et al. [7] for the free (F) case. For the sake of clarity, the reference solutions are not shown in Fig. 2; it suffices to simply point out that the current results match very well with them in every case. In the guided and free cases, the first modes represent rigid body motions whose radiation efficiencies were previously studied by Swenson and Johnson [32]. Although the modal radiation efficiencies for some lower-order modes appear to be not very sensitive to the boundary conditions, the corresponding natural frequencies are actually significantly different from one case to another (Table 1), which implies that the radiated power will be meaningfully altered by the edge supports. This notion will be further elaborated below.

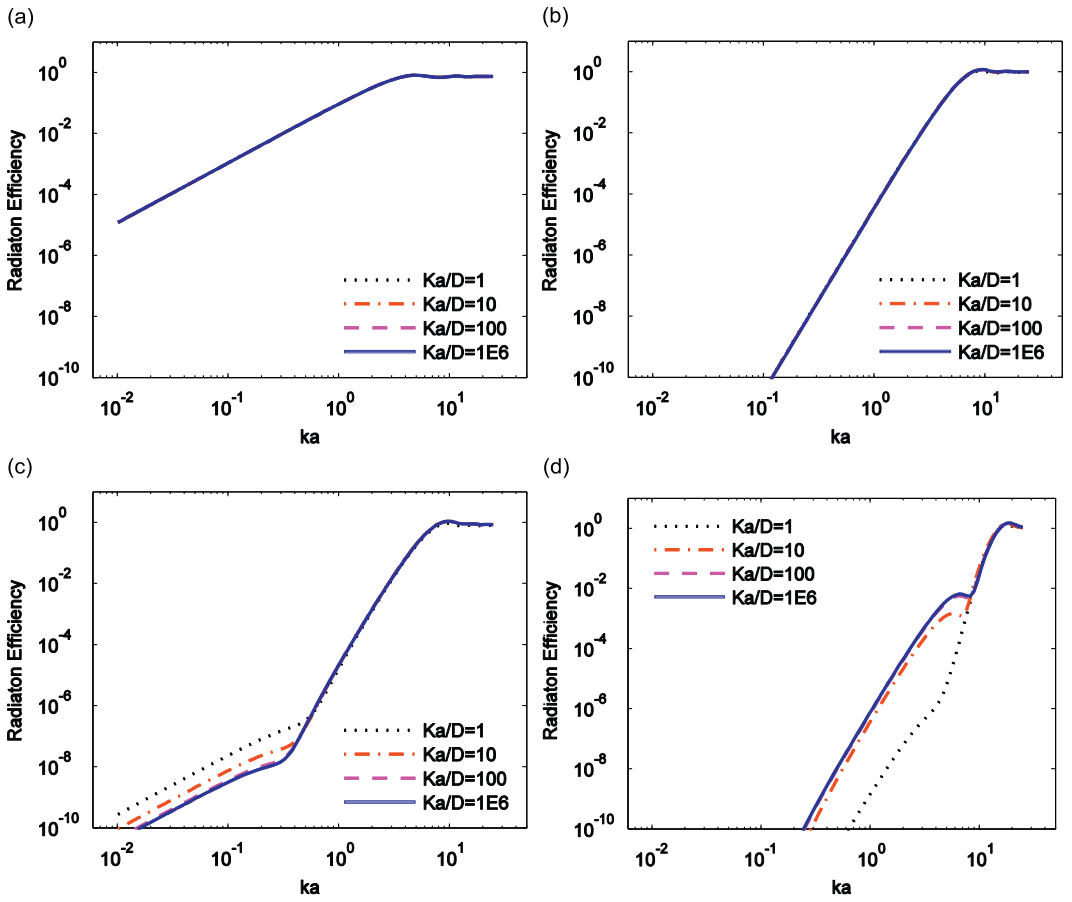

Fig. 3. The modal radiation efficiencies for the (a) 1st, (b) 4th, (c) 5th, and (d) 20th modes of a rectangular plate (r=1.2) with a constant restraint against deflection (ka^3/D=1) and the varying levels of restraints against rotation.

4.2. Modal radiation efficiencies for plates with elastic boundary supports

Next we consider a few cases in which each edge of the plate is elastically restrained against both deflection and rotation. First, the stiffness of the transverse spring is held as constant, ka^3/D=1, and the rotational spring takes different stiffness values: Ka/D=1, 10, 100, and 10^6. Plotted in Fig. 3 are the radiation efficiencies for several "randomly" selected modes. It is seen that although the rotational restraints have little effect on the radiation efficiencies for the 1st and 4th modes, they can meaningfully modify the acoustic characteristics of the higher-order modes such as the 5th and 20th modes. However, there seem to be no clear correlations between the restraining stiffness and the (up- or downward) shifts of the radiation efficiency curves.

Now the stiffness of the rotational springs is kept as constant, Ka/D=1, and the stiffness for the transverse springs is chosen as ka^3/D=1, 10, 100, and 10^6. Fig. 4 shows the modal radiation efficiencies for the 1st, 4th, 5th, and 14th modes. Obviously, the modal radiation efficiencies are relatively more sensitive to the stiffness of the transverse springs. In particular, the radiation efficiencies for the 1st and 4th modes have been noticeably increased as the stiffness decreases. This is understandable from that fact that for $ka^3/D=10^6$ and Ka/D=1, the plate is essentially simply supported with a moderate level of rotational restraints. Thus, as the transverse restraints are weakened, the plate tends to move more "freely" and "uniformly" in the transverse direction, which results in an increase of the piston-like portion in the mode shapes. The relatively larger active area will make the corresponding modes radiate more effectively than their counterparts in the simply supported case. It should be noted that since the modal radiation efficiencies are normalized by the mean-square velocities of the corresponding modes, the amount of the piston-like motion in each mode, which depends on the stiffness of the transverse restraints, tends not to have a significant effect (as manifested in the overlap of the radiation efficiency curves in Fig. 4(a, b)). An opposite trend is observed for the 5th mode which indicates that the allowance of the piston-like motion may also neutralize the radiation effectiveness of the edges or corners in some modes. In comparison, the effects of the restraining stiffness on the radiation efficiencies of higher-order modes, such as the 20th mode, appear to be "unpredictable" regarding the (up- or downward) shift directions. This problem may be understood from a different angle; that is, when the boundary condition becomes significantly different from the baseline, the modal properties will be modified accordingly such that the modal index can no longer be safely used for modal pairing.

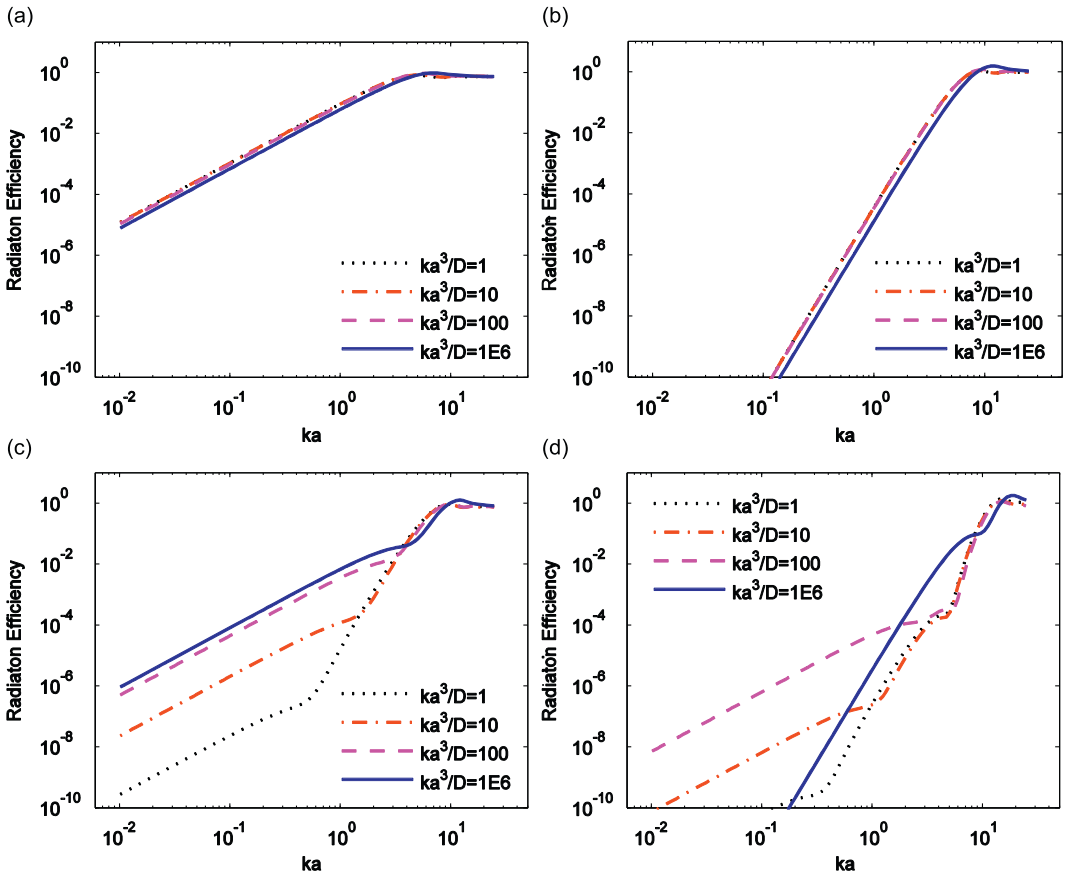

Fig. 4. The modal radiation efficiencies for the (a) 1st, (b) 4th, (c) 5th, and (d) 20th modes of a rectangular plate (r=1.2) with a constant restraint against rotation (Ka/D=1) and the varying levels of restraints against deflection.

4.3. Acoustic powers radiated from plates with different clamping configurations

In order to avoid the difficulty of dealing with several variables simultaneously, all four edges are subjected to the same elastic restraint in the problems discussed above. In the current model, however, each edge can be independently and arbitrarily restrained. Due to a large number of scenarios possible for structural (including boundary conditions) modifications, the task for achieving a specific acoustic design goal is better conducted under the framework of design optimization or sensitivity study. In what follows, however, we will attempt to understand how the sound power radiation can be affected by the number of the restrained edges. If we take a fully clamped (CCCC) square plate as the baseline configuration and consider three boundary condition modifications (CCCF, CCFF, and CFFF) by freeing one edge at a time. The modal radiation efficiencies for several selected modes (the 1st, 2nd, 3rd, 4th, 14th, and 20th modes) are shown in Fig. 5 for these different boundary conditions. The modal radiation efficiencies are almost the same for the first modes in all these cases. However, the radiation efficiencies for the other modes vary considerably from one case to another.

The sound power radiated from the plate is calculated by assuming that a unit point force is applied to the center of the plate. A uniform structural damping, η=0.02, is used in the calculations. The results are plotted in Fig. 6 for all four boundary conditions. The peaks on the sound power curves are directly correlated with the natural frequencies of the plate. For clarity, the radiated powers are shown separately for each boundary condition. However, the difference between them can still be clearly observed, indicating that the acoustic behavior of a plate can be meaningfully influenced by its boundary condition. The question of how to properly select and install a panel to reduce its sound radiation is of direct interest to noise control engineers. Understandably, such a decision will also depend on a number of other factors or criteria in practice. However, it is noteworthy that the radiation behavior of a planar source can be meaningfully affected by the boundary condition; thus, the proposed model provides a useful means to make appropriate structural modifications.

5. Conclusions

A general method has been developed for the analysis of the acoustic radiation from a rectangular plate with each of its edges being arbitrarily supported by elastic restraints against both deflection and rotation. Any uniform or non-uniform

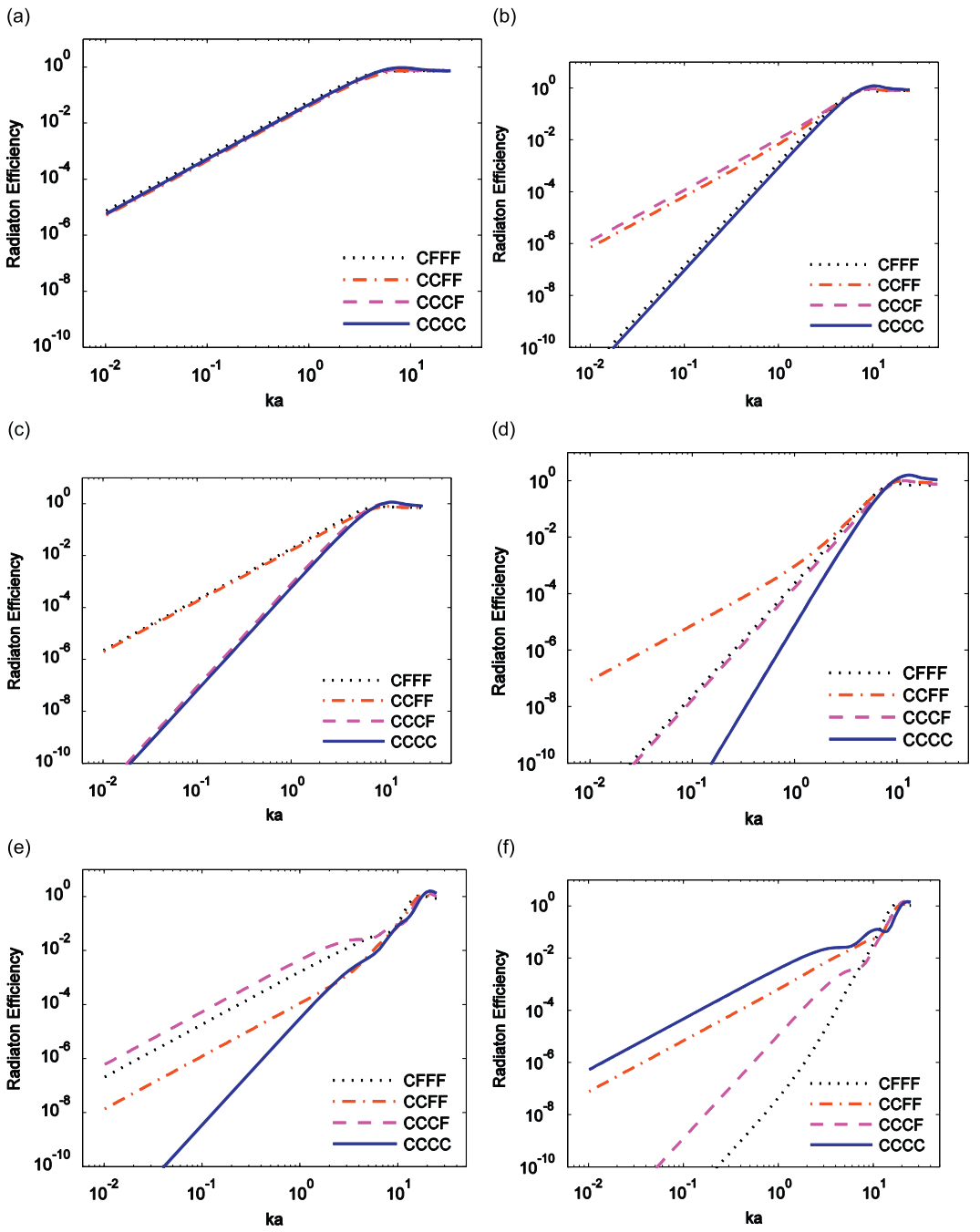

Fig. 5. The modal radiation efficiencies for the (a) 1st, (b) 2nd, (c) 3rd, (d) 4th, (e) 14th, and (f), 20th modes of a rectangular plate (r=1.2) under different clamping schemes.

boundary conditions can be directly taken into account by specifying the stiffness distributions accordingly. The displacement function in the vibration analysis is invariably sought as a modified Fourier series expansion that is subsequently reduced to a standard two-dimensional Fourier cosine series to facilitate the acoustic calculations. This has two immediate advantages. First, the sound radiation from rectangular plates, regardless of the boundary conditions or structural details, can be universally determined from the radiation resistances for an invariant and complete set of basic functions in the form of cosine functions. Thus, the computing-intensive acoustic calculations need to be carried out only once when a plate is subjected to a number of structural and/or boundary condition modifications. Second, the present

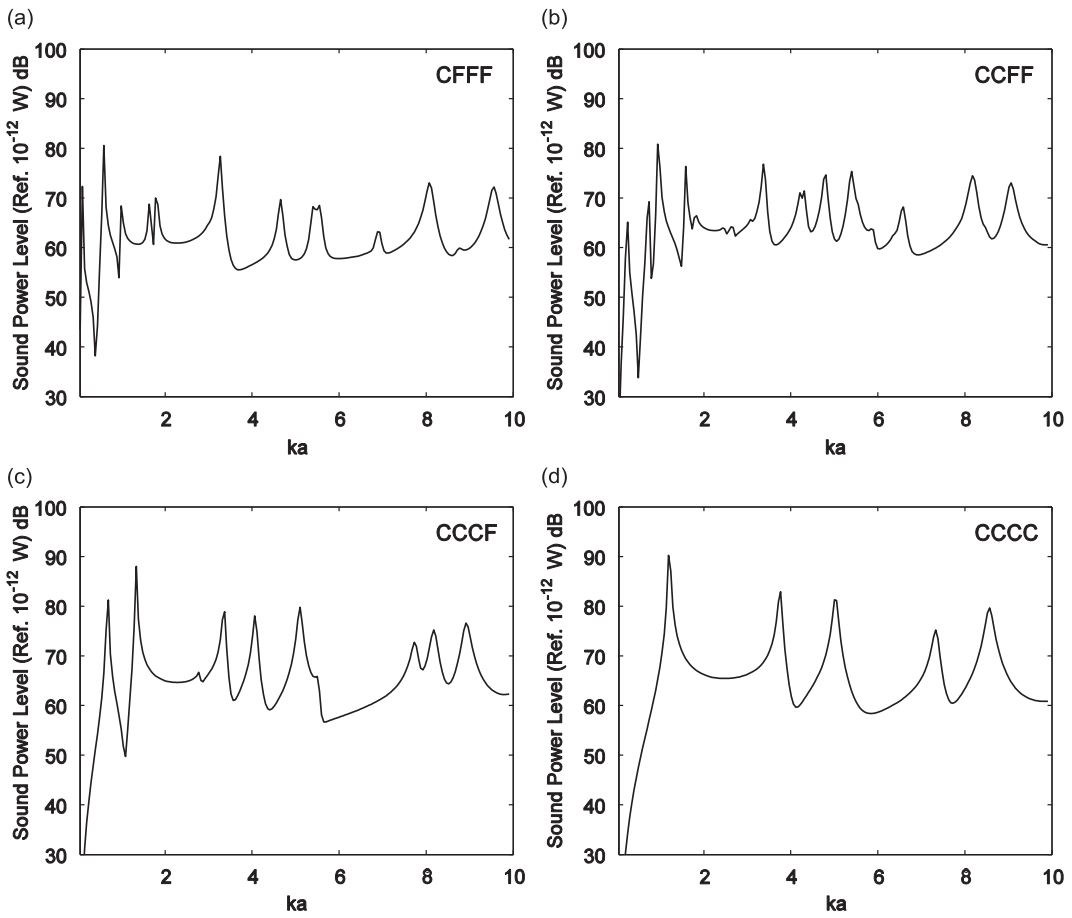

Fig. 6. Sound powers radiated from a rectangular plate (r=1.2) under (a) CCCC, (b) CCCF, (c) CCFF, and (d) CFFF boundary conditions.

formulation potentially provides a hybrid analytical–experimental means for determining the sound power (radiated from a planar source) based on the measured vibration data. In such an approach, the Fourier coefficients will be directly obtained from a Discrete Cosine Transform (DCT) of the displacement or velocity data measured on the surface of the source.

An analytical expression in the form of the power series of the non-dimensional acoustic wavenumber has been derived for an effective determination of the "universal" radiation resistance matrix. Although this formula is mathematically accurate and valid for any wavenumber, it should be practically limited to $ka < 25$ in actual calculations to avoid a possible numerical breakdown due to computer round-off errors. By taking the acoustic wavenumber ka as abscissa, each radiation efficiency curve will then only depend upon the aspect ratio of a plate, which makes it possible to calculate the radiation resistance matrices off-line and save them for later uses.

The present method has been numerically validated by the results previously obtained by other researchers. Numerical examples are also presented to demonstrate that the modal radiation efficiencies of a plate can be meaningfully modified by changing its boundary conditions. Modal radiation efficiencies are also calculated for plates with elastically restrained edges. It appears that the modal radiation efficiencies are relatively more sensitive to the stiffness of transverse restraints. Finally, the radiated sound powers are compared for a plate under four different clamping schemes. It has been demonstrated that the boundary conditions can have a significant impact on the modal radiation efficiencies and the radiated sound powers. Thus, modifying the boundary conditions potentially represents an effective and practical means for tuning the acoustic characteristics of a planar source.

Acknowledgment

The authors gratefully acknowledge the financial support from NSF Grant: CMMI-0827233.

Appendix A. Additional definitions

The new variables in Eqs. (20)–(22)) are defined as follows:

$$\begin{aligned}\mathrm{I}(a,b,m,n,m',n',x,y) = D\left[\lambda_{am}^4+\lambda_{bn}^4+2\lambda_{am}^2\lambda_{bn}^2\right]\Delta_m\Delta_n\delta_{mm'}\delta_{nn'}\\ +\frac{1}{2}\left(k_{x_0,n+n'}+k_{x_0,|n-n'|}+(-1)^{m'+m}\left(k_{x_a,n+n'}+k_{x_a,|n-n'|}\right)\right)\\ +\frac{1}{2}\left(k_{y_0,m+m'}+k_{y_0,|m-m'|}+(-1)^{n'+n}\left(k_{y_b,m+m'}+k_{y_b,|m-m'|}\right)\right),\end{aligned} \tag{A1}$$

$$\begin{aligned}\mathrm{II}(j,a,b,m,n,m',x,\beta) = D\left[(\lambda_{am}^4+\nu\lambda_{am}^2\lambda_{bn}^2)\beta_n^j-(\lambda_{bn}^2+\nu\lambda_{am}^2)\overline{\overline{\beta}}_n^j-2(1-\nu)\lambda_{bn}\lambda_{am}^2\overline{\beta}_n^j\right]\Delta_m\delta_{mm'}\\ +\frac{1}{2}\sum_{l=0}^{\infty}(\tilde{k}_{x_0,l}+\tilde{k}_{x_a,l}(-1)^{m+m'})(\beta_{n+l}^j+\beta_{|n-l|}^j)\\ +\frac{1}{2}\left[\xi_b^j(0)(k_{y_0,m+m'}+k_{y_0,|m-m'|})+\xi_b^j(b)(-1)^n(k_{y_b,m+m'}+k_{y_b,|m-m'|})\right],\end{aligned} \tag{A2}$$

$$\begin{aligned}\mathrm{III}(i,j,a,b,m,m',x,y,\beta) = D\left[\lambda_{am}^4\beta_{i,j}^{0,0}+\beta_{i,j}^{2,2}-\nu\lambda_{am}^2(\beta_{i,j}^{2,0}+\beta_{i,j}^{0,2})\right.\\ \left.+2(1-\nu)\lambda_{am}^2\beta_{i,j}^{1,1}\right]\Delta_m\delta_{mm'}+\sum_{l=0}^{\infty}\left(\tilde{k}_{x_0,l}+\tilde{k}_{x_a,l}(-1)^{m+m'}\right)\beta_{i,j,l}^{0,0}\\ +\frac{1}{2}\left[\xi_b^i(0)\xi_b^j(0)(k_{y_0,m+m'}+k_{y_0,|m-m'|})+\xi_b^i(b)\xi_b^j(b)(k_{y_b,m+m'}+k_{y_b,|m-m'|})\right]\\ +\frac{1}{2}\left[\xi_b'i(0)\xi_b'j(0)(K_{y_0,m+m'}+K_{y_0,|m-m'|})+\xi_b'i(b)\xi_b'j(b)(K_{y_b,m+m'}+K_{y_b,|m-m'|})\right],\end{aligned} \tag{A3}$$

$$\begin{aligned}\mathrm{IV}(i,j,a,b,m,n',x,y,\alpha,\beta) = D\left[-\lambda_{am}^2\overline{\overline{\alpha}}_m^j\beta_{n'}^i-\lambda_{bn'}^2\alpha_m^j\overline{\overline{\beta}}_{n'}^i+\nu\overline{\overline{\alpha}}_m^j\overline{\overline{\beta}}_{n'}^i+\nu\lambda_{am}^2\lambda_{bn'}^2\beta_{n'}^i\alpha_m^j+2(1-\nu)\lambda_{am}\lambda_{bn'}\overline{\beta}_{n'}^i\overline{\alpha}_m^j\right]\\ +\frac{1}{2}\sum_{l=0}^{\infty}(\tilde{k}_{x_0,l}\xi_a^j(0)+\tilde{k}_{x_a,l}(-1)^m\xi_a^j(a))(\beta_{n'+l}^i+\beta_{|n'-l|}^i)\\ +\frac{1}{2}\sum_{s=0}^{\infty}(\tilde{k}_{y_0,s}\xi_b^i\nu+\tilde{k}_{y_b,s}(-1)^{n'}\xi_b^i(b))(\alpha_{m+s}^j+\alpha_{|m-s|}^j),\end{aligned} \tag{A4}$$

$$\mathrm{V}(m,n,m',n') = \Delta_m\Delta_n\delta_{mm'}\delta_{nn'}, \quad \mathrm{VI}(j,m,n,m',\beta) = \Delta_m\beta_n^j\delta_{mm'}, \tag{A5, A6}$$

$$\mathrm{VII}(i,j,m,m',\beta) = \Delta_m\beta_{i,j}^{0,0}\delta_{mm'} \quad \text{and} \quad \mathrm{VIII}(i,j,m,n') = \alpha_m^j\beta_{n'}^i, \tag{A7, A8}$$

where

$$\Delta_m = \int_0^a(\cos\lambda_{am}x)^2\,\mathrm{d}x = (1+\delta_{m0})a/2, \quad \alpha_m^j = \int_0^a\xi_a^j(x)\cos\lambda_{am}x\,\mathrm{d}x, \quad \overline{\alpha}_m^j = \int_0^a\xi_a'j(x)\sin\lambda_{am}x\,\mathrm{d}x$$

$$\overline{\overline{\alpha}}_m^j = \int_0^a\xi''^j{}_a(x)\cos\lambda_{am}x\,\mathrm{d}x, \quad \alpha_{i,j}^{0,0} = \int_0^a\xi_a^i(x)\xi_a^j(x)\,\mathrm{d}x, \quad \alpha_{i,j}^{0,2} = \int_0^a\xi_a^i(x)\xi''^j{}_a(x)\,\mathrm{d}x,$$

$$\alpha_{i,j}^{2,0} = \int_0^a\xi''^i{}_a(x)\xi_a^j(x)\,\mathrm{d}x \quad \alpha_{i,j}^{2,2} = \int_0^a\xi''^i{}_a(x)\xi''^j{}_a(x)\,\mathrm{d}x, \quad \alpha_{i,j,m}^{0,0} = \int_0^a\xi_{ia}(x)\xi_{ja}(x)\cos\lambda_{am}x\,\mathrm{d}x,$$

$$\tilde{\alpha}_m^j = \alpha_m^j/\Delta_m, \quad k_{x_0,n} = \int_0^a k_{x_0}(y)\cos\lambda_{bn}y\,\mathrm{d}y, \quad K_{x_0,n} = \int_0^a K_{x_0}(y)\cos\lambda_{bn}y\,\mathrm{d}y, \quad \tilde{k}_{x_0,n} = k_{x_0,n}/\Delta_n, \quad \text{and}$$

$$\tilde{K}_{x_0,n} = K_{x_0,n}/\Delta_n$$

Their counterparts, Δ_n, β_n^j, $\overline{\beta}_n^j$, $\overline{\overline{\beta}}_n^j$, $\beta_{i,j}^{0,0}$, $\beta_{i,j}^{0,2}$, $\beta_{i,j}^{2,0}$, $\beta_{i,j}^{2,2}$, $\beta_{i,j,l}^{0,0}$, $\tilde{\beta}_n^j$, $k_{y0,m}$, $K_{y0,m}$, $\tilde{k}_{y_0,m}$, and $\tilde{K}_{y_0,m}$, can be defined in a similar manner.

$$K_{mn,m'n'}^{11} = \mathrm{I}(a,b,m,n,m',n',x,y), \tag{A9}$$

$$K_{mn,jm'}^{12} = \mathrm{II}(j,a,b,m,n,m',x,\beta), \quad K_{im,m'n'}^{21} = \mathrm{II}(i,a,b,m,n',m',x,\beta), \tag{A10, A11}$$

$$K_{mn,jn'}^{13} = \mathrm{II}(j,b,a,n,m,n',y,\alpha), \quad K_{in,m'n'}^{31} = \mathrm{II}(i,b,a,n,m',n',y,\alpha), \tag{A12, A13}$$

$$K_{im,jm'}^{22} = \mathrm{III}(i,j,a,b,m,m',x,y,\beta), \quad K_{in,jn'}^{33} = \mathrm{III}(i,j,b,a,n,n',y,x,\alpha), \tag{A14, A15}$$

$$K_{im,jn'}^{23} = \mathrm{IV}(i,j,a,b,m,n',x,y,\alpha,\beta), \quad K_{in,jm'}^{32} = \mathrm{IV}(i,j,b,a,n,m',y,x,\beta,\alpha), \tag{A16, A17}$$

$$M^{11}_{mn,m'n'} = V(m,n,m',n'), \tag{A18}$$

$$M^{12}_{mn,jm'} = \mathrm{VI}(j,m,n,m',\beta), \quad M^{21}_{im,m'n'} = \mathrm{VI}(i,m,n',m',\beta), \tag{A19, A20}$$

$$M^{13}_{mn,jn'} = \mathrm{VI}(j,n,m,n',\alpha), \quad M^{31}_{in,m'n'} = \mathrm{VI}(i,n,m',n',\alpha), \tag{A21, A22}$$

$$M^{22}_{im,jm'} = \mathrm{VII}(i,j,m,m',\beta), \quad M^{33}_{in,jn'} = \mathrm{VII}(i,j,n,n',\alpha), \tag{A23, A24}$$

$$M^{23}_{im,jn'} = \mathrm{VIII}(i,j,m,n'), \quad M^{32}_{in,jm'} = \mathrm{VIII}(j,i,m',n), \tag{A25, A26}$$

$$f_{mn} = \int_0^a \int_0^b f(x,y)\cos\lambda_{am}x\cos\lambda_{bn}y\,\mathrm{d}x\,\mathrm{d}y, \tag{A27}$$

$$f^i_{am} = \int_0^a \int_0^b f(x,y)\xi^i_b(y)\cos\lambda_{am}x\,\mathrm{d}x\,\mathrm{d}y, \tag{A28}$$

and

$$f^i_{bn} = \int_0^a \int_0^b f(x,y)\xi^i_a(x)\cos\lambda_{bn}y\,\mathrm{d}x\,\mathrm{d}y. \tag{A29}$$

References

[1] S. Snyder, N. Tanaka, Calculating total acoustic power output using modal radiation efficiencies, *Journal of the Acoustical Society of America* 97 (1995) 1702–1709.
[2] J. Park, L. Mongeau, T. Siegmund, Influence of support properties on the sound radiated from the vibrations of rectangular plates, *Journal of Sound and Vibration* 264 (2003) 775–794.
[3] K.A. Cunefare, Effect of modal interaction on sound radiation from vibrating structures, *American Institute of Aeronautics and Astronautics Journal* 30 (1992) 2819–2828.
[4] M.C. Gomperts, Sound radiation from baffled, thin, rectangular plates, *Acoustica* 37 (1977) 93–102.
[5] G. Maidanik, Response of ribbed panels to reverberant acoustic fields, *Journal of the Acoustical Society of America* 34 (1962) 809–826.
[6] F.G. Leppington, E.G. Broadbent, K.H. Heron, The acoustic radiation efficiency of rectangular panels, *Proceedings of The Royal Society of London, Series A* 382 (1982) 245–271.
[7] A. Berry, J.L. Guyader, J. Nicolas, A general formulation for the sound radiation from rectangular, baffled plates with arbitrary boundary conditions, *Journal of the Acoustical Society of America* 88 (1990) 2792–2802.
[8] H.G. Davies, Sound from turbulent-boundary-layer-excited panels, *Journal of the Acoustical Society of America* 49 (1971) 878–889.
[9] C.E. Wallace, Radiation resistance of a baffled beam, *Journal of the Acoustical Society of America* 51 (1972) 936–945.
[10] C.E. Wallace, Radiation resistance of a rectangular panel, *Journal of the Acoustical Society of America* 51 (1972) 946–952.
[11] H. Levine, On the short wave acoustic radiation from planar panels or beams of rectangular shape, *Journal of the Acoustical Society of America* 76 (1984) 608–615.
[12] R.F. Keltie, H. Peng, The effects of modal coupling on the acoustic power radiation from panels, *Journal of Vibration, Acoustics, Stress, and Reliability in Design* 109 (1987) 48–54.
[13] W.L. Li, H.J. Gibeling, Acoustic radiation from a rectangular plate reinforced by springs at arbitrary locations, *Journal of Sound and Vibration* 220 (1999) 117–133.
[14] W.L. Li, H.J. Gibeling, Determination of the mutual radiation resistances of a rectangular plate and their impact on the radiated sound power, *Journal of Sound and Vibration* 229 (2000) 1213–1233.
[15] W.L. Li, An analytical solution for the self and mutual radiation resistances of a rectangular plate, *Journal of Sound and Vibration* 245 (2001) 1–16.
[16] W.R. Graham, Analytical approximations for the modal acoustic impedances of simply supported, rectangular plates, *Journal of the Acoustical Society of America* 122 (2007) 719–730.
[17] F.G. Leppington, E.G. Broadbent, F.R. S, K.H. Heron, Acoustic radiation from rectangular panels with constrained edges, *Proceedings of The Royal Society of London, Series A* 393 (1984) 67–84.
[18] F.J. Fahy, Vibration of containing structures by sound in the contained fluid, *Journal of Sound and Vibration* 10 (1969) 490–512.
[19] M. Ohlrich, C.T. Hugin, On the influence of boundary constraints and angled baffle arrangements on sound radiation from rectangular plates, *Journal of Sound and Vibration* 277 (2004) 405–418.
[20] N.S. Lomas, S.I. Hayek, Vibration and acoustic radiation of elastically supported rectangular plates, *Journal of Sound and Vibration* 52 (1977) 1–25.
[21] W.L. Li, Vibroacoustic analysis of rectangular plates with elastic rotational edge restraints, *Journal of the Acoustical Society of America* 120 (2006) 769–779.
[22] M.C. Gomperts, Sound radiation from baffled, thin, rectangular plates with general boundary conditions, *Acoustica* 30 (1974) 946–952.
[23] O. Beslin, J. Nicolas, A hierarchical functions set for predicting very high order plate bending modes with any boundary conditions, *Journal of Sound and Vibration* 202 (1997) 633–655.
[24] H. Nelisse, O. Beslin, J. Nicolas, A generalized approach for the acoustic radiation from baffled or unbaffled plate with arbitrary boundary conditions, immersed in a light or heavy fluid, *Journal of Sound and Vibration* 211 (1998) 207–225.
[25] W.L. Li, X. Zhang, J. Du, Z. Liu, An exact series solution for the transverse vibration of rectangular plates with general elastic boundary supports, *Journal of Sound and Vibration* 321 (2009) 254–269.
[26] G.P. Tolstov, *Fourier Series*, Prentice-Hall, Englewood Cliffs, NJ, 1965.
[27] C. Lanczos., *Discourse on Fourier Series*, Hafner, New York, 1966.
[28] W.B. Jones, G. Hardy, Accelerating convergence of trigonometric approximations, *Mathematics of Computation* 24 (1970) 547–560.
[29] G. Baszenski, F.-J. Delvos, M. Tasche, A united approach to accelerating trigonometric expansions, *Computers and Mathematics with Applications* 30 (1995) 33–49.
[30] X. Zhang, W.L. Li, Vibrations of rectangular plates with arbitrary non-uniform elastic edge restraints, *Journal of Sound and Vibration* 326 (2009) 221–234.
[31] E.G. Williams, A series expansion of the acoustic power radiated from planar sources, *Journal of the Acoustical Society of America* 73 (1983) 1520–1524.
[32] G.W. Swenson, W.E. Johnson, Radiation impedance of a rigid square piston in an infinite baffle, *Journal of the Acoustical Society of America* 24 (1952) 84.